Aerosol and Air Quality Research, 18: 1221–1235, 2018

ISSN: 1680-8584 print / 2071-1409 online
doi: 10.4209/aaqr.2017.10.0394

Spatio-temporal Variations in NO_2 and $PM_{2.5}$ over the Central Plains Economic Region of China during 2005-2015 Based on Satellite Observations

Kun Cai[1,2], Shenshen Li[3*], Fengbin Zheng[2], Chao Yu[3], Xueying Zhang[4], Yang Liu[2], Yujing Li[2]**

[1] *College of Environment and Planning, Henan University, Kaifeng 475004, China*
[2] *College of Computer and Information Engineering, Henan University, Kaifeng 475004, China*
[3] *State Key Laboratory of Remote Sensing Science, Institute of Remote Sensing and Digital Earth, Chinese Academy of Sciences, Beijing 100101, China*
[4] *Department of Epidemiology, Human Genetics and Environmental Sciences, School of Public Health, The University of Texas Health Science Center at Houston, Houston, TX 77030, USA*

ABSTRACT

The Central Plains Economic Region (CPER) is located in central eastern China and has experienced tremendous economic growth in the last decade. Like many areas in China, the rapid economic development of the CPER has led to serious air pollution problems, including extremely high concentrations of nitrogen dioxide (NO_2) and particulate matter with an aerodynamic diameter less than 2.5 µm ($PM_{2.5}$). However, the current air pollution monitoring system lacks good spatial and temporal coverage. Therefore, we used high-resolution satellite remote sensing techniques to analyze the variation in NO_2 and $PM_{2.5}$ in the CPER from 2005 through 2015. The Ozone Monitoring Instrument (OMI) and the Moderate Resolution Imaging Spectroradiometer (MODIS) were used to retrieve the tropospheric NO_2 columns and ground-level $PM_{2.5}$ concentrations, respectively. High NO_2 and $PM_{2.5}$ concentrations were mainly located in the central and northern areas of the CPER. The highest 11-year average concentrations were found in the city of Jiaozuo for NO_2 (19.54×10^{15} molecules cm^{-2}) and in the city of Hebi for $PM_{2.5}$ (107.8 µg m^{-3}). The western and southern mountainous areas had lower NO_2 and $PM_{2.5}$ concentrations. The average seasonal NO_2 and $PM_{2.5}$ concentrations were both highest in winter and lowest in summer. The average monthly concentrations of NO_2 and $PM_{2.5}$ were as high as 24.60×10^{15} molecules cm^{-2} and 152.2 µg m^{-3}, respectively, in January 2013 and as low as 43.86×10^{15} molecules cm^{-2} and 40.2 µg m^{-3}, respectively, in July 2006. During the 11-year study period (2005–2015), the CPER concentrations of both NO_2 and $PM_{2.5}$ decreased from 2011 to 2015 by 31.5% and 36.8%, respectively. This study successfully applies satellite remote sensing data to quantitatively analyze the spatial-temporal distributions of tropospheric NO_2 and ground-level $PM_{2.5}$. This approach can support air pollution monitoring in the CPER, and the estimated concentrations can provide references for environmental policymaking.

Keywords: $PM_{2.5}$; NO_2; CPER; OMI; MODIS.

INTRODUCTION

In recent decades, China has experienced both rapid economic development and dramatic growth of air pollution problems. Living in one of the most polluted countries, nearly all of China's population of 1.3 billion resides in areas that do not meet the World Health Organization (WHO)'s Air Quality Guidelines (AQG) of 10 µg m^{-3} (Apte *et al*., 2015; Ma *et al*., 2015; Van Donkelaar *et al*., 2015; West *et al*., 2016). Nitrogen dioxide (NO_2) and particulate matter with an aerodynamic diameter less than 2.5 µm ($PM_{2.5}$) are the two major air pollutants in China (Streets *et al*., 2013).

The environmental effects of ambient NO_2 have received considerable attention. To reduce the environmental damage associated with acidification, eutrophication and ozone depletion, the United Nations European Economic Commission (UNECE) issued the Sofia Agreement in 1988 and the Goteborg Protocol in 1999 to reduce the emissions of NO_2 by human activities. In the United States, both nitrogen oxide (NO_x) emissions and ambient NO_x concentrations were reduced by approximately 30% from 1990 to 2006 (United States Environmental Protection

* Corresponding author.
Tel.: 086+13718051982
E-mail address: lishenshen@126.com
** Corresponding author.
Tel.: 086+13592126211
E-mail address: zhengfb@henu.edu.cn

Agency (USEPA), 2010). Compared to developed countries, China was late in initiating control of NO_2 emissions. In 2010, only 18% of China's power plants were using denitrification technology to reduce NO_2 emissions (Wang and Hao, 2012). Previous studies have analyzed the long-term NO_x trends in China. For example, Zhao *et al.* (2013) showed that the NO_x emissions in China increased rapidly from 11.0 Mt in 1995 to 26.1 Mt in 2010. De Foy *et al.* (2016) suggested that there was an increase in Ozone Monitoring Instrument (OMI)-retrieved NO_2 columns in most areas from 2005 to approximately 2011, which was followed by a strong decrease continuing through 2015. Gu *et al.* (2013) found large regional, seasonal, and urban/rural variations in NO_x emission trends based on an analysis of OMI observations of NO_2 columns over China from 2005 to 2010. Meanwhile, studies have shown that the concentrations of NO_2 in China have rapidly increased because of the development of large industries and a greater number of motor vehicles in the recent decade (van der A *et al.*, 2006; Zhang *et al.*, 2007).

$PM_{2.5}$ particles can directly enter human alveoli and can cause adverse health effects (Duki *et al.*, 2003; Pope and Dockery, 2006). In addition, China's high $PM_{2.5}$ concentrations have received global attention (Wang *et al.*, 2014b). Van Donkelaar *et al.* (2006) showed that the North China Plain was the area with the highest concentrations of $PM_{2.5}$ in the world. According to the "China Environmental Status Bulletin 2014," the average concentration of $PM_{2.5}$ in China was 62 μg m^{-3}, and few Chinese cities met the WHO's air quality standard (10 μg m^{-3} as an annual mean) in the statistical year of 2012.

In 2012, NO_2 and $PM_{2.5}$ were added to the Chinese Ambient Air Quality Standard as criteria air pollutants. The Ministry of Environmental Protection (MEP) of China started to publish the monitored mass concentrations of NO_2 and $PM_{2.5}$ at each China Environmental Monitoring Center (CEMC) located in major Chinese cities in January 2013 (Wang *et al.*, 2014a; Zhang and Cao, 2015; Zhao *et al.*, 2016). However, the monitored data might not be representative because of the limited number and spatial distribution of monitors. For example, most monitors were located in urban areas; hence, those monitors provided inadequate information about the air pollution in rural areas, where the air quality was still likely to be affected by industrial complexes. In addition, the earliest date of air pollution data we could access from the China's monitoring system was in 2013. Thus, historical air pollution data are not available for continental China.

The understanding of the spatial distribution of air pollution in China has been recently improved by the application of advanced assessment tools, such as satellite remote sensing. Satellite-retrieved products have many advantages, including global coverage, high spatial-temporal resolution, and historical datasets (Zhang *et al.*, 2004). The application of satellite remote sensing in retrieving tropospheric NO_2 columns and predicting ground-level $PM_{2.5}$ has become a popular research area. Zhou *et al.* (2015, 2016a, b) analyzed the temporal and spatial variations in NO_2 concentrations and the relevant influential factors in the Beijing-Tianjin-Hebei district, Yangtze River Delta, and Shandong regions using the OMI product. Zhang *et al.* (2017b) used OMI data to analyze the temporal and spatial changes in the column concentrations of NO_2 and SO_2 in Henan Province over the past decade. Yao and Lu (2014) used the Moderate Resolution Imaging Spectroradiometer (MODIS) aerosol optical depth (AOD) to estimate the distribution of $PM_{2.5}$ concentrations in China from 2006 through 2010. Sun *et al.* (2017) retrieved 1-km MODIS AOD in the Beijing-Tianjin-Hebei region to analyze the spatial and temporal distribution of aerosols. Ma *et al.* (2016) combined the MODIS AOD and the two-step generalized additive model approach to estimate the ground-level $PM_{2.5}$ concentration in China for the study year 2004–2013. Therefore, the application of satellite remote sensing has extended the assessment of air pollution to areas without monitors.

The Central Plains Economic Region (CPER) is located in central eastern China. With a population of 160 million, the CPER is one of the most populous areas in the world. The intense consumption of fossil fuels driven by the large population and rapid economic growth has led to a serious air pollution problem in the CPER. The economic growth of the CPER ranks fourth behind the Yangtze River Delta, the Pearl River Delta, and the Beijing-Tianjin-Hebei region in recent years. In addition, the CPER is an area that has one of the highest coal consumption rates in China (Li *et al.*, 2012). As noted by the Civil Aviation Administration of China (CAAC)'s air quality report in 2015, the majority of the CPER was classified as a heavily polluted area in terms of $PM_{2.5}$ (CAAC, 2015). The air pollution of the CPER was ranked as the second worst in China in terms of the concentration of $PM_{2.5}$ pollution, behind the Beijing-Tianjin-Hebei district (Natural Resources Defense Council (NRDC), 2015). The cities of Xingtai, Zhengzhou, Anyang, and Handan within the CPER have frequently been ranked among the top 10 most polluted cities in China. In 2017, China's MEP implemented an emission control program to reduce the air pollution in Beijing, Tianjin and 26 other heavily polluted cities in China, and the program was referred to as the "2+26" program (Ministry of Environmental Protection, 2017). Nine cities in the CPER were included in the "2+26" program, and monitoring and emission reductions were strengthened in order to reduce the concentrations of NO_2 and $PM_{2.5}$ in the air.

Determining the air pollution in the CPER is of great importance because the air quality of the CPER is likely affected by many factors. First, the CPER's air pollution represents a mixture of natural sources and anthropogenic sources. Second, the CPER is near two major economic zones in China, the Beijing-Tianjin-Hebei region and the Yangtze River Delta. The transport of air pollutants between economic zones may have a large impact on the air pollution level in the CPER. Nevertheless, the current air pollution monitoring network has a poor spatial resolution, and no historical data prior to 2013 are available. Therefore, we used satellite data to retrieve tropospheric NO_2 columns and ground-level $PM_{2.5}$ concentrations at a high spatial resolution in the CPER domain. By incorporating factors that influence air pollution and statistical models, we are

able to estimate the source impact of NO_2 and $PM_{2.5}$ from 2005 through 2015. The approaches we used in this study can provide exposure assessment results for air quality management and policymaking in the CPER.

DATA AND METHODS

Study Area

The CPER is an economic development zone covering the entire administrative area of Henan Province and surrounding areas. As shown in Fig. 1, the CPER, located in central China (110°E–118°E, 32°N–38°N), has a total area of approximately 2.89×10^5 km^2 and contains 28 cities in five provinces (i.e., Henan, Shandong, Anhui, Hebei, and Shanxi). In addition, the Central Plains Urban Agglomeration (CPUA) consists of 12 cities within the CPER (i.e., Zhengzhou, Luoyang, Kaifeng, Xinxiang, Jiaozuo, Xuchang, Pingdingshan, Luohe, Jiyuan, Hebi, Shangqiu, and Zhoukou). In particular, Zhengzhou, as a key connection center for China's high-speed rail network, is an important ground transportation hub and has experienced greater economic growth than other cities in the CPER.

OMI-retrieved NO_2

The OMI is a sensor installed on the Aura satellite, which was launched by the U.S. National Aeronautics and Space Administration (NASA) in July 2004. The OMI was co-produced by the Netherlands, Finland and NASA (Celarier *et al.*, 2008). It was designed to detect trace gases in the atmosphere and to study the roles that trace gases play in climate change. The orbit of the OMI is sun-synchronous and has a swath as wide as approximately 2600 km. The products of the OMI have a spatial resolution of 13 km × 24 km and daily retrieval (Boersma *et al.*, 2007; Wenig *et al.*, 2008). Thus, these products can be used to measure the daily concentrations of trace gases at high spatial resolution. In this study, the satellite product used to measure the ground-level NO_2 concentrations was the monthly average tropospheric NO_2 column dataset (DOMINO version 2.0) obtained from the Tropospheric Emission Monitoring Internet Service (TEMIS) (http://www.temis.nl/airpollution/no2.html). This product is a level-3 OMI product and was globally gridded at a spatial resolution of 0.125°. The OMI NO_2 data provided by this product were the tropospheric vertical column density data, which is labeled VCD_NO_2 (or simply NO_2) and represents the total number of NO_2 molecules, and these data were further processed to seasonal and annual averages for investigation. Similar to the popular NASA NO_2 product, the DOMINO product is also based on the differential optical absorption spectroscopy (DOAS) algorithm. The differences between the DOMINO and NASA products include different methods for adjusting the stratospheric contribution and the use of different terrain and profile datasets for conversion of the tropospheric slant column into a vertical column (Russell *et al.*, 2012). DOMINO subtracts stratospheric contributions as determined by a data assimilation system, while the NASA product estimates stratospheric NO_2 from OMI data without using stratospheric chemical transport models directly. Additionally, DOMINO calculates the air mass factor (AMF) with a priori NO_2 monthly mean vertical profile shapes from the Global Modeling Initiative (GMI) model (Bucsela *et al.*, 2013). Despite the differences, both algorithms produce statistically similar regional trends (Krotkov *et al.*, 2016). Ialongo *et al.* (2016) found that the retrieval uncertainties render these two products indistinguishable.

Several studies have validated the OMI-retrieved NO_2 by using ground-based measurements in China. For example, Lin *et al.* (2014) validated the DOMINO NO_2 columns by using ground-based MAX-DOAS measurements in China. Linear regression yields a correlation coefficient (R^2) of 0.73, a slope of 0.98, and an error within 30%. Jin *et al.* (2016) found that the correlation coefficient between OMI-retrieved and ground-measured NO_2 concentrations was 0.95 for the North China Plain. Zhang *et al.* (2017a) compared the OMI-retrieved NO_2 concentrations with the ground concentrations of NO_2 measured at 24 monitoring

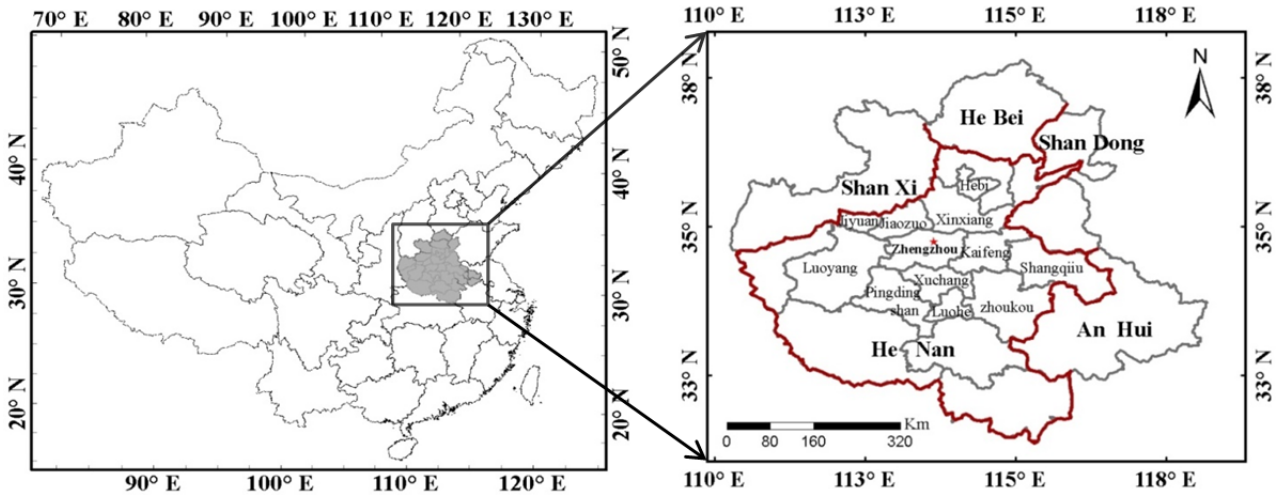

Fig. 1. The location of the study area (CPER) in China. Henan Province is outlined in red. The twelve cities of the Central Plains Urban Agglomeration (CPUA) are located in northern Henan Province.

sites in Beijing. Their findings revealed consistent positive correlations across all sites, and the overall R^2 was 0.92. Notably, lightning in the upper troposphere can produce 10–20% of the NO_x generated on a global scale (Miyazaki *et al.*, 2014). However, in China, previous studies (Guo *et al.*, 2016; 2017) found that the annual mean contribution of lightning to the total tropospheric NO_x is only 7.5%. Furthermore, the lightning contribution is even lower in eastern China than in western China. Therefore, the effect of lightning on NO_x emissions over the CPER is assumed to be negligible in this study. Considering that the DOMINO product has been widely used in many studies on NO_2 emissions trends (Irie *et al.*, 2016; Liu *et al.*, 2016), we believe that choosing the DOMINO NO_2 product will not cause a substantial change in our results.

MODIS-estimated $PM_{2.5}$

We followed the two-stage approach developed by Ma *et al.* (2016) to estimate the daily-level $PM_{2.5}$ concentrations using satellite-retrieved AOD in the CPER for 2005–2015. The first stage of the statistical model adopted a linear mixed-effect model, which was adjusted with the monitored $PM_{2.5}$ concentrations and the same grid cell's AOD, as well as with meteorological factors collected from weather stations near the grid cell. The second stage adopted a generalized additive model, which used a smoothing function to optimize the land-use parameters and geographical coordinates to improve the model's performance in predicting $PM_{2.5}$.

In this model, the AOD data were generated using the dark target algorithm from MODIS. The process of the MODIS Level 2.0 AOD product has been described at length by its development group (Levy *et al.*, 2013). The level-2 products with 10-km-resolution AOD data were downloaded from the Atmosphere Archive and Distribution System database (LAADS web: https://ladsweb.modaps.eosdis.nasa.gov/) for the study period 2005–2015. The ground-based $PM_{2.5}$ data used for model fitting were obtained from the website of the CEMC for all available $PM_{2.5}$ sites located inside the CPER. Overall, data were collected from more than 150 sites. We matched the AOD values to the ground-level measurements of $PM_{2.5}$ concentrations in the same 10-km grid cell and on the same day that the $PM_{2.5}$ data were collected. This model also used meteorological parameters, such as planetary boundary layer (PBL) height, relative humidity (RH), wind speed, and surface pressure, from the Goddard Earth Observing System Data Assimilation System (GEOS-5), as well as 300-m-resolution land use data from the European Space Agency Land Cover data portal (http://due.esrin. esa.int/page_globcover.php).

Ma *et al.* (2016) has validated the two-stage model $PM_{2.5}$ data using the corresponding ground-based observations throughout China. For example, the correlation between satellite and in situ measurements in 2014 in China was 0.85; seasonally, this correlation was 0.89. Our approach here also involved a focused validation study to illustrate the applicability of the estimated $PM_{2.5}$ data from the two-stage statistical model over the study area. Fig. 2 is a scatterplot of the monthly averaged $PM_{2.5}$ concentrations from ground-based observations and MODIS-estimated $PM_{2.5}$ concentrations during 2013–2015. Overall, the satellite estimates have a strong correlation with the ground-based data ($y = 0.71x + 27.96$, $r = 0.77$). Therefore, the two-stage statistical model can reliably estimate historical $PM_{2.5}$ data and effectively reflect the concentration levels of the near-ground $PM_{2.5}$ in the research area.

RESULTS AND ANALYSIS

Spatial distributions of NO_2 and $PM_{2.5}$ in the CPER

The spatial distributions of NO_2 and $PM_{2.5}$ concentrations in the CPER are shown in Fig. 3. As shown in Fig. 3(b), the high NO_2 concentrations were mainly found in relatively developed and populous areas, such as Zhengzhou, northern Luoyang, Jiaozuo, Jiyuan, western Xinxiang, northern

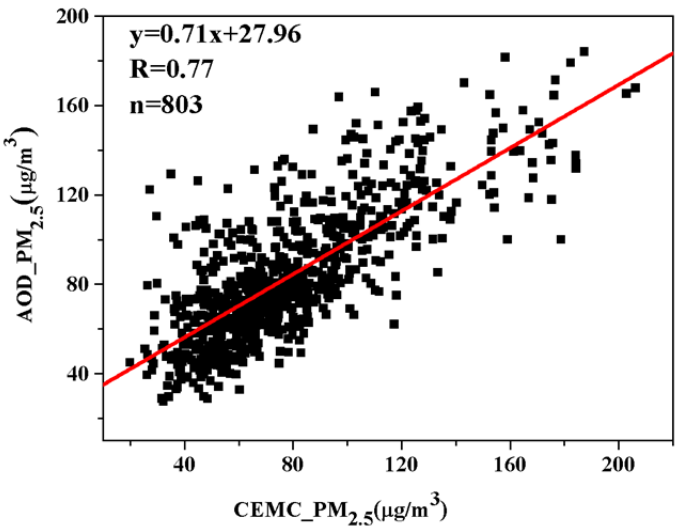

Fig. 2. Scatterplot of the monthly averaged $PM_{2.5}$ concentrations from the China Environmental Monitoring Center (CEMC) and MODIS-estimated $PM_{2.5}$ during 2013–2015.

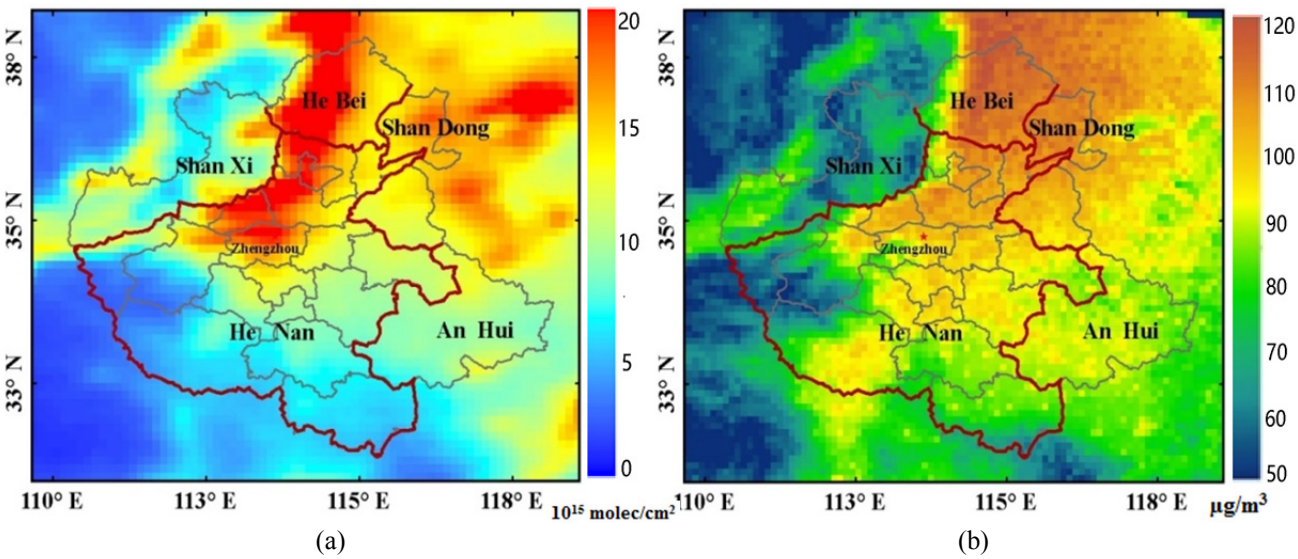

Fig. 3. Spatial distributions of the 11-year averaged NO_2 and $PM_{2.5}$ concentrations in the CPER during 2005–2015: (a) NO_2 columnar concentration based on OMI DOMINO products at 0.125° × 0.125° resolution and (b) $PM_{2.5}$ mass concentration based on MODIS-estimated at 0.1° × 0.1° resolution.

Anyang, and eastern Hebei Province. In addition, high concentrations of NO_2 were also found in areas with high industrial emissions. For example, Jiaozuo has the highest average concentration of NO_2, and it is also the location of the largest coal mine in central China. The NO_2 concentrations in the mountainous areas of western and southern Henan were estimated to be lower than those in the cities, which may be due to the high vegetation coverage and the lack of anthropogenic emissions.

As shown in Fig. 3(b), the distribution of $PM_{2.5}$ concentrations exhibited great spatial variation. The annual average concentrations of $PM_{2.5}$ in our study were consistent with the measured $PM_{2.5}$ concentrations in the cities with air monitors. The cities ranked by air quality from worst to best are Zhengzhou, Kaifeng, Xuchang, Luohe, southwestern Luoyang, Jiaozuo, Xinxiang, Hebi, Anyang, and Puyang. Across the CPER domain, high $PM_{2.5}$ concentrations mainly occurred along the southern side of the Taihang Mountains and in areas with perennially dominant northeast and southwest winds. These topographical and meteorological conditions prevent air pollutants from dispersing, resulting in an accumulation of air pollutants on the southern side of the Taihang Mountains (Tian *et al.*, 2011). The areas with relatively low concentrations of $PM_{2.5}$ included the city of Sanmenxia, which is located in western Henan Province, and southwestern Luoyang and Xinyang, which are located in southern Henan Province and Shanxi Province, respectively.

The twelve core cities in the CPUA serve as the industrial and economic center of the CPER and were also the most polluted areas in the CPER. Therefore, a statistical analysis of the concentrations of NO_2 and $PM_{2.5}$ in these twelve cities in the CPUA was performed (Tables 1 and 2). In the results, Luoyang had the lowest average concentrations of both NO_2 (7.74×10^{15} molecules cm^{-2}) and $PM_{2.5}$ (75.5 μg m^{-3}) during the 11 study years. Jiaozuo had the highest NO_2 concentration (19.54×10^{15} molecules cm^{-2}), and Hebi had the highest $PM_{2.5}$ concentration (107.8 μg m^{-3}) among the 12 CPUA cities.

The two major causes of the air pollution in the CPUA cities were the high density of industrial facilities and difficulty dispersing the air pollution due to their geographic locations. For example, the economy of the city with the highest NO_2 concentrations for the 11 study years, Jiaozuo, relies heavily on coal mining and metallurgical industry. According to Henan Province's Governmental Statistics, although Jiaozuo contained only 3.7% of Henan Province's population, it contributed 5.2% of the province's total gross domestic product (GDP) and 7.1% of the province's industrial production in the year 2015. During the same year, although the GDP contributed by Hebi was not as high as that of Jiaozuo, 62% of the city's GDP was contributed by heavy industry, such as automotive manufacturing. Hebi built two large power plants (a 2,200-MW thermal power plant and a 4,100-MW coal-fired power plant) to provide electricity for the heavy industry facilities, and both of the power plants consumed large amounts of fossil fuels, consequently releasing large amounts of air pollution into the city. In addition to containing areas with the highest air pollution levels in China, Hebei Province also acted as a source of air pollutants to nearby cities, lowering their air quality (Wang *et al.*, 2007).

Monthly and Seasonal Patterns of NO_2 and $PM_{2.5}$ in the CPER

The spatial distributions of the monthly average concentrations of NO_2 and $PM_{2.5}$ in the CPER over the 11 study years are shown in Figs. 4 and 5, respectively. As shown in Fig. 4, January and December had higher NO_2 concentrations than the other months. Throughout almost all of the CPER, the NO_2 concentrations were highest (NO_2 > 15×10^{15} molecules cm^{-2}) in January and December, and

Table 1. The mean (plus standard deviation) NO_2 concentrations (10^{15} molecules cm^{-2}) for the twelve cities in the CPUA during 2005–2015.

City	2005	2006	2007	2008	2009	2010	2011	2012	2013	2014	2015	Average
Jiaozuo	16.68(7.29)	16.23(6.16)	20.30(7.49)	20.53(7.08)	20.64(8.47)	22.74(9.48)	24.09(12.47)	22.14(9.58)	21.07(8.59)	16.56(9.91)	13.96(7.93)	19.54(3.17)
Hebi	14.53(6.67)	16.03(7.09)	19.98(10.48)	18.39(10.03)	18.27(9.84)	19.88(7.61)	22.67(12.84)	22.70(10.54)	25.49(16.46)	16.28(8.91)	14.06(8.18)	18.93(3.49)
Xinxiang	14.02(7.52)	13.80(6.62)	17.79(9.56)	18.04(10.85)	18.00(11.54)	20.08(9.03)	21.10(12.22)	19.46(9.45)	21.48(13.36)	15.28(9.41)	13.05(7.68)	17.46(3.04)
Zhengzhou	13.74(6.50)	13.15(5.56)	16.90(7.36)	15.78(6.53)	16.43(7.16)	19.13(8.56)	20.97(9.64)	18.63(8.40)	20.31(12.58)	15.31(8.03)	12.42(6.50)	16.62(2.96)
Jiyuan	10.19(4.21)	11.04(4.68)	12.93(5.97)	12.69(3.31)	14.53(8.38)	15.66(5.78)	16.69(8.58)	15.16(7.24)	16.45(8.80)	12.94(8.40)	9.45(5.66)	13.43(2.47)
Kaifeng	9.94(6.27)	8.98(4.85)	12.11(9.04)	12.56(8.81)	12.31(8.68)	14.10(8.47)	14.69(9.88)	14.66(8.76)	17.30(17.36)	10.47(6.75)	10.23(6.33)	12.49(2.53)
Xuchang	10.09(5.36)	9.29(4.46)	13.18(7.20)	11.53(5.41)	12.49(6.71)	13.57(7.89)	15.78(9.46)	14.51(8.10)	15.09(12.27)	11.67(7.31)	9.88(5.34)	12.46(2.22)
Shangqiu	10.30(7.26)	8.71(4.67)	11.12(8.48)	10.96(7.99)	10.13(6.99)	11.31(8.29)	13.29(9.36)	14.02(9.39)	12.78(9.59)	9.55(6.36)	8.51(6.02)	10.97(1.80)
Luohe	7.77(4.91)	7.08(3.89)	9.71(6.27)	9.00(4.86)	9.35(5.31)	9.88(6.55)	13.16(9.43)	11.16(6.47)	12.11(12.65)	8.79(5.89)	8.07(4.78)	9.64(1.89)
Zhoukou	8.43(6.40)	6.82(3.69)	10.00(7.57)	8.86(5.46)	8.33(5.28)	9.57(7.57)	11.57(8.78)	11.84(7.84)	12.47(12.12)	8.16(6.86)	7.88(5.48)	9.45(1.82)
Pingdingshan	7.40(3.50)	6.99(3.51)	9.51(4.66)	8.32(3.10)	9.34(5.14)	9.39(5.14)	11.93(6.51)	10.13(5.87)	10.32(6.91)	8.55(5.60)	6.56(3.63)	8.95(1.62)
Luoyang	6.22(2.70)	6.43(3.31)	7.90(3.88)	7.32(2.72)	7.73(4.90)	8.4(4.72)	9.66(4.91)	8.98(6.26)	9.11(5.45)	7.73(5.05)	5.63(3.31)	7.74(1.32)

Table 2. The mean (plus standard deviations) $PM_{2.5}$ concentrations ($\mu g\ m^{-3}$) for the twelve cities in the CPUA during 2005–2015.

City	2005	2006	2007	2008	2009	2010	2011	2012	2013	2014	2015	Average
Hebi	101.0(41.58)	114.9(37.04)	110.7(32.56)	108.7(38.04)	111.5(34.07)	109.5(35.82)	112.2(32.93)	119.2(43.02)	117.5(46.30)	96.8(30.53)	83.5(18.50)	107.8(10.23)
Xinxiang	98.6(44.31)	109.1(34.88)	109.0(34.97)	106.0(39.53)	105.6(35.35)	107.5(36.94)	111.9(36.89)	114.6(39.85)	112.7(47.03)	90.8(29.99)	81.0(20.15)	104.3(10.33)
Jiaozuo	99.2(39.16)	105.4(37.31)	105.2(31.24)	102.5(30.63)	103.2(31.30)	104.7(33.87)	115.3(35.52)	113.3(42.51)	112.4(45.63)	83.7(30.05)	75.5(19.13)	101.9(12.13)
Kaifeng	93.5(41.70)	100.8(31.12)	105.7(39.57)	100.5(37.53)	101.0(34.15)	105.1(36.77)	110.0(34.02)	112.6(38.18)	108.0(51.78)	86.9(29.82)	78.9(20.40)	100.3(10.35)
Luohe	92.6(36.77)	100.4(36.46)	108.0(38.38)	96.7(37.51)	100.6(37.40)	105.4(39.41)	112.7(41.36)	107.5(40.63)	100.8(50.32)	77.1(23.62)	73.0(20.73)	97.7(12.56)
Zhengzhou	92.0(39.15)	100.1(29.93)	100.3(32.10)	96.8(29.65)	97.6(33.06)	101.1(33.83)	110.1(36.27)	106.5(41.19)	102.8(46.62)	80.4(25.77)	75.1(20.41)	96.6(10.27)
Xuchang	93.0(40.94)	99.0(32.44)	103.2(36.97)	95.0(33.76)	97.5(36.78)	101.7(40.65)	109.4(41.03)	107.1(39.59)	100.9(53.27)	79.0(25.30)	74.4(20.55)	96.4(11.51)
Zhoukou	88.0(37.94)	92.4(35.51)	103.5(41.10)	94.4(38.12)	99.0(34.99)	99.8(38.38)	107.0(40.13)	104.1(37.02)	94.0(46.02)	77.4(25.26)	71.9(21.33)	93.8(10.94)
Shangqiu	85.8(36.63)	92.7(34.21)	100.8(38.98)	92.8(38.95)	96.0(36.08)	97.7(37.60)	102.2(36.62)	103.9(35.58)	93.2(41.78)	79.8(25.52)	72.2(22.04)	92.5(9.63)
Pingdingshan	89.4(38.12)	95.5(31.50)	95.0(31.02)	91.1(34.42)	91.4(35.03)	95.2(36.44)	101.6(37.03)	99.7(38.59)	96.0(49.70)	68.5(23.08)	66.6(19.12)	90.0(12.03)
Jiyuan	87.4(36.14)	92.1(36.36)	90.1(28.17)	85.9(22.87)	88.4(26.37)	87.7(30.48)	96.8(31.05)	95.8(39.56)	97.2(42.76)	70.7(30.89)	65.4(19.11)	87.0(12.14)
Luoyang	76.9(34.78)	80.6(29.50)	79.1(25.80)	76.3(28.49)	77(29.20)	78.1(30.33)	84.2(32.18)	82.6(34.54)	81.7(38.78)	57.9(19.44)	55.7(16.50)	75.5(9.46)

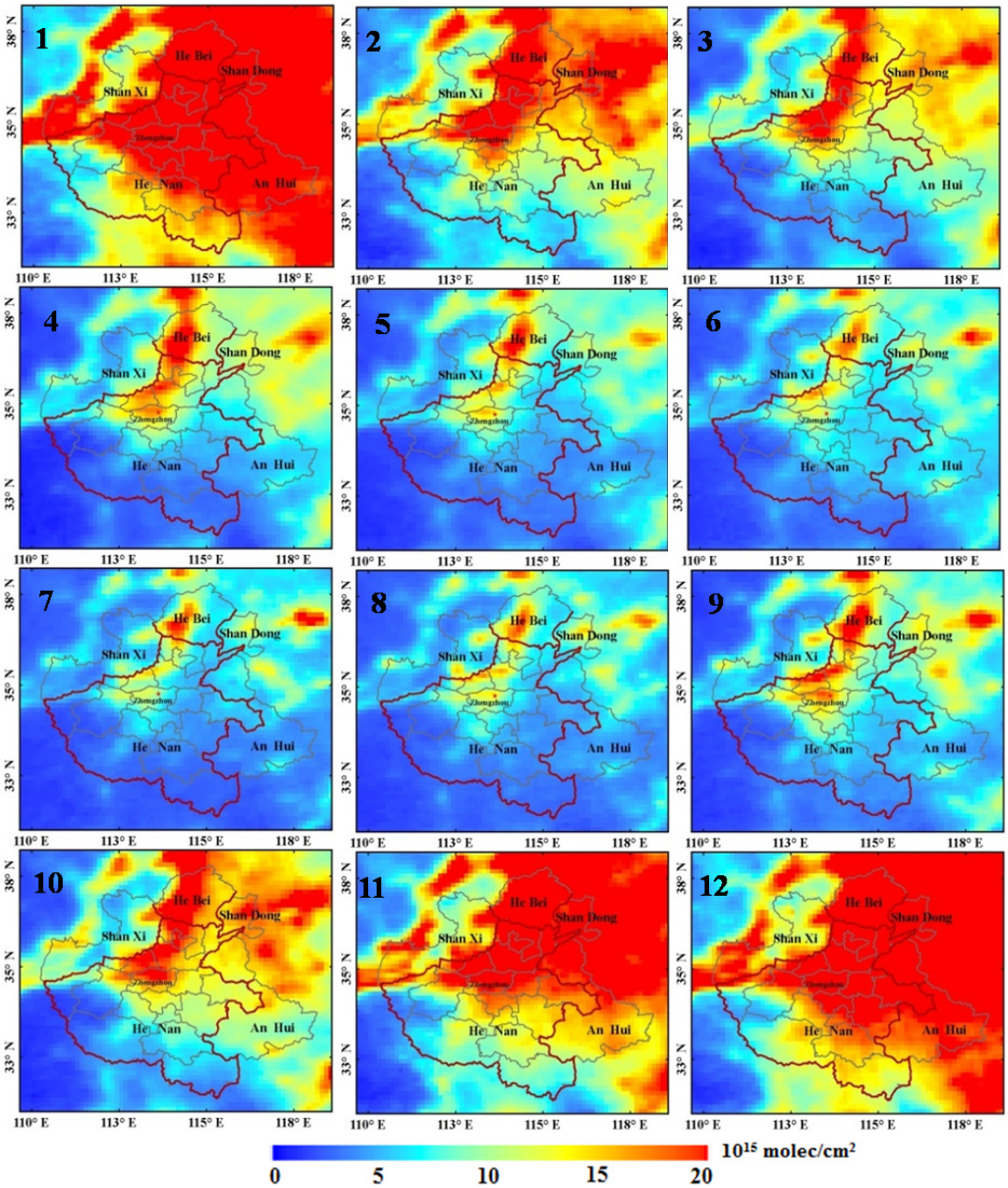

Fig. 4. Monthly average NO_2 columnar concentration distributions in the CPER during 2005–2015 based on OMI DOMINO products at 0.125° × 0.125° resolution.

the highest concentrations were mainly distributed in northern and central-eastern CPER. From January to February, the predicted concentrations of NO_2 decreased in the northern CPER. In the middle and late spring (March and April), the area with high predicted concentrations narrowed down to individual cities, such as Jiaozuo, Zhengzhou, Hebi, and Anyang in Henan Province and Handan and Xingtai in Hebei Province. The overall NO_2 level was relatively lower and less varied during May to August than in the other months. The NO_2 concentrations increased in September and October, as shown by the expanded areas with high concentrations in Fig. 4. The NO_2 concentrations increased as winter arrived. The highest level of NO_2 concentrations expanded greatly from October to November in Fig. 4, and the northern CPER had greater increases than the southern CPER in terms of the expanded area with high NO_2 concentrations.

The variation in the monthly average concentrations of $PM_{2.5}$ was similar to that of NO_2 across the different months (Fig. 5). The $PM_{2.5}$ concentrations were higher in the months of December, January and February than in the other months. Fig. 5 showed that almost the entire domain

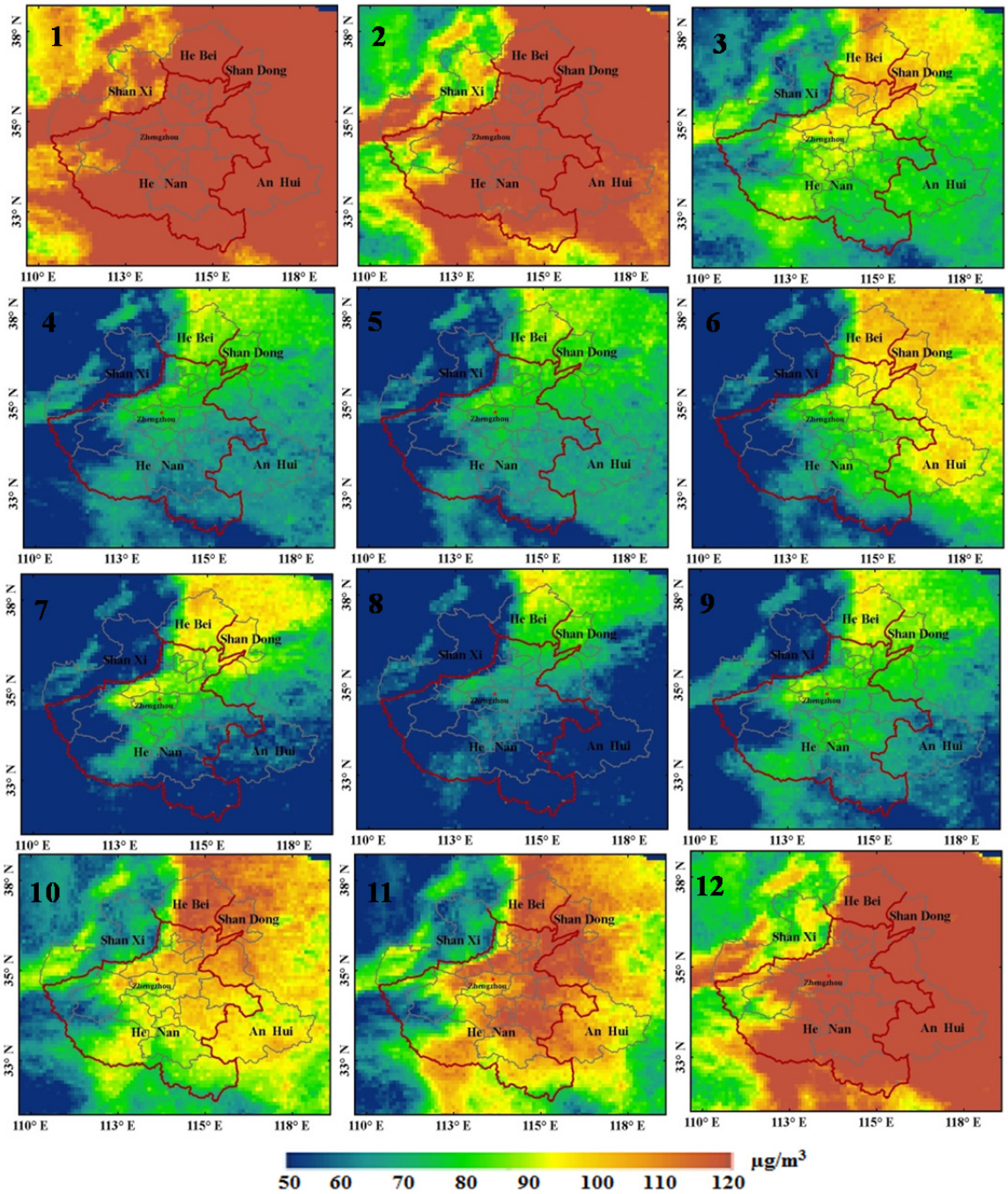

Fig. 5. Monthly average $PM_{2.5}$ mass concentration distributions in the CPER during 2005–2015 based on MODIS-estimated at 0.1° × 0.1° resolution.

of the CPER was in the highest category for $PM_{2.5}$ ($PM_{2.5}$ > 100 μg m^{-3}). The $PM_{2.5}$ concentrations decreased in March, as shown by the decrease in the area of high $PM_{2.5}$ concentrations in Fig. 5. Only Zhengzhou and northern Kaifeng were above the lowest level of $PM_{2.5}$. The $PM_{2.5}$ concentrations continued to decrease in April and May, and the decreases were greater in Sanmenxia and in the western, mountainous area of Luoyang. The variations in $PM_{2.5}$ concentrations were not consistent across different CPER areas and were not straightforward in different summer months (June, July, and August). In June and July, the predicted concentrations of $PM_{2.5}$ increased greatly in the northern and middle areas of the CPER. In addition to the widespread occurrence of crop residue burning, the increase in aerosols might be due to the relatively strong solar radiation in summer, which can promote more rapid photochemical reactions by accelerating the transformation of NO_2 to NO_3^- and SO_2 to SO_4^{2-}. On one hand, these transformations reduce the lifetime of gas-phase air pollutants in the atmosphere, but on the other hand, they also cause high concentrations of nitrate and sulfate particles (Wang *et al.*, 2011; Zhang *et al.*, 2012; Cheng *et al.*, 2013). In

August, the predicted concentrations of $PM_{2.5}$ decreased in most areas in Henan Province, and the lowest values were found in the western and southern regions of Henan Province and in northern Shanxi Province (red polygon in Fig. 5). From September to November, the areas with high predicted concentrations of $PM_{2.5}$ expanded from individual cities to the majority of the eastern CPER. The increase in $PM_{2.5}$ concentrations in the late fall might be associated with straw burning in Henan Province. The widespread grain farmlands in Henan Province leave thousands of tons of straw in the field after the harvest. Because no appropriate alternative crop waste management approach is available, this farmland straw is incinerated. The burning straw is a major source of $PM_{2.5}$ and other air pollutants (e.g., SO_2, NO_x, and VOC) in the late fall and early winter period in central China. A previous study has shown that the concentrations of inhalable particles near farmlands were three times higher than usual during the straw burning period (Li *et al.*, 2008).

The seasonal variations in the NO_2 concentrations and the $PM_{2.5}$ concentrations are shown in Fig. 6. The seasonal patterns of NO_2 and $PM_{2.5}$ found in our study were consistent with the seasonal patterns of NO_2 and $PM_{2.5}$ reported in other studies. The concentrations of NO_2 and $PM_{2.5}$ were generally higher in the fall and winter seasons. In addition to the high precursor emissions due to heating and coal burning, the wintertime adverse weather conditions also contribute significantly to the high surface $PM_{2.5}$ concentrations in the CPER. For example, the PBL height over the North China Plain is usually less than 500 m in winter (Li *et al.*, 2016), resulting in less efficient vertical transport and mixing of particles to higher altitudes. In addition, the limited precipitation in the cold season hinders the wet deposition of $PM_{2.5}$, so high concentrations of air pollutants can remain in the atmosphere for a longer time. Compared to the $PM_{2.5}$ concentrations, the NO_2 concentrations exhibited a greater decrease from winter to summer. During the summer season, the atmospheric temperatures and humidity were relatively high, which accelerated the oxidization process of NO_2 in the air (Khoder, 2002). In addition, the CPER features a warm temperate subtropical climate. The frequent rainfall in the summer season greatly reduced the NO_2 concentrations in the atmosphere (Yan *et al.*, 2015).

The seasonal variations in NO_2 concentrations and $PM_{2.5}$ concentrations varied among the different areas in the CPER (Fig. 6). Zhengzhou, Jiaozuo, Xinxiang, Hebi, and Anyang are all located in northern Henan Province, and Handan and Xingtai are located in southern Hebei Province. During the spring (Fig. 6(a)), the NO_2 concentrations in these regions were high, and the $PM_{2.5}$ concentrations were generally low. During the summer (Fig. 6b), most regions had low NO_2 concentrations, but Zhengzhou, Jiaozuo, Xinxiang, Handan, and Xingtai, which formed the center of the developed area, had higher concentrations. The $PM_{2.5}$ concentrations showed two prominent low-value areas in the western and southern mountain regions. During the autumn (Fig. 6(c)), the high-concentration area was widespread, with high NO_2 concentrations in the northern region and high $PM_{2.5}$ concentrations extending over a large area of the central eastern section of the study region. During the winter (Fig. 6(d)), most regions still showed high NO_2 concentrations. Additionally, the concentrations decreased from north to south and from east to the west, and the concentrations of $PM_{2.5}$ across the entire province were high, except over Pingdingshan, the mountainous area of Luoyang in Henan Province, and northern Shanxi Province.

Eleven-year Variations in NO_2 and $PM_{2.5}$ in the CPER

Fig. 7 shows the 11-year variations (2005–2015) in the

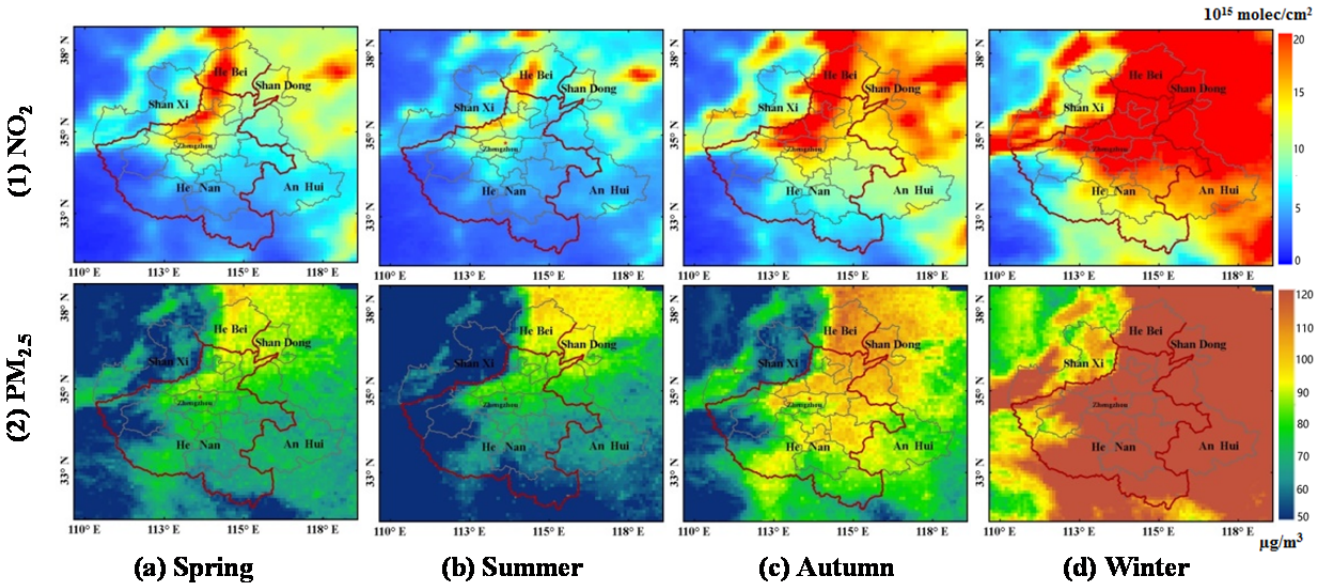

Fig. 6. Seasonally averaged NO_2 and $PM_{2.5}$ distributions in the CPER during 2005–2015: (1) NO_2 columnar concentration based on OMI DOMINO products at 0.125° × 0.125° resolution and (2) $PM_{2.5}$ mass concentration based on MODIS-estimated at 0.1° × 0.1° resolution; (a) Spring, (b) Summer, (c) Autumn, and (d) Winter.

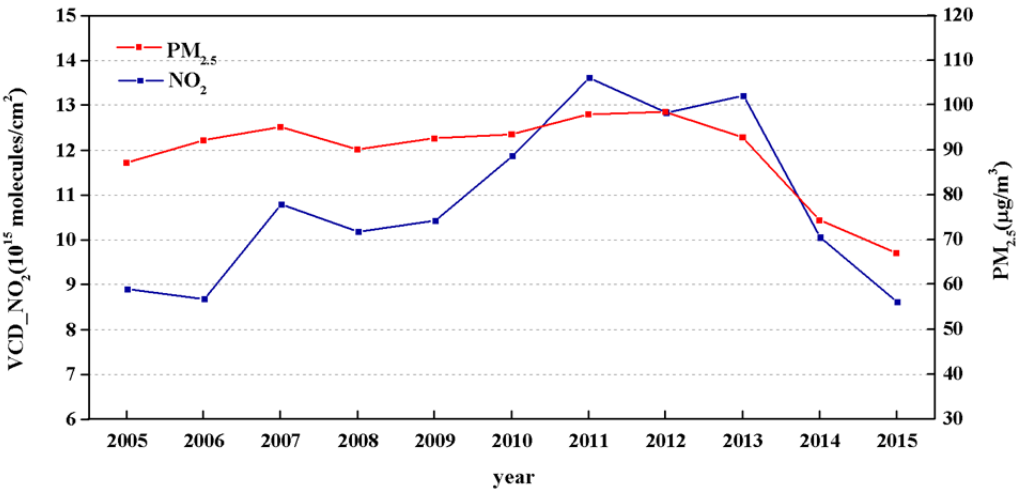

Fig. 7. The annual variations in NO_2 columnar concentration and $PM_{2.5}$ mass concentration in the CPER during 2005–2015.

NO_2 and $PM_{2.5}$ concentrations in the CPER. Overall, the variations in NO_2 were greater than those in $PM_{2.5}$, but the trends were similar between the two pollutants. As shown in Fig. 7, the concentrations of NO_2 and $PM_{2.5}$ increased from 2005 to 2011 and then decreased after 2011. Our results before 2011 are consistent with the findings of Itahashi *et al.* (2014), who concluded that there was an increase in OMI NO_2 columns during 2000–2010 in central eastern China. The rapid growth in NO_2 column density before 2011 was driven by the increase in anthropogenic NO_x emissions in China (Zhao *et al.*, 2013). For example, the total capacities of coal-fired power generation increased by 48.8% in 2005–2007 (Wang *et al.*, 2012). The turning point of NO_2 and $PM_{2.5}$ concentrations in the year 2011 may be related to the Chinese government's "12th Five-Year Plan", which included policies related to emission reductions to control serious air pollution. As a result, the national NO_2 level has decreased by 6% year^{-1} since 2011 (Irie *et al.*, 2016). In Henan Province, industrial NO_2 emissions amounted to 719,500 tons in 2015, which was 28% lower than that in 2010. Correspondingly, the NO_2 concentration in Henan Province decreased by 27.4% during those five years. Although there was no reduction plan directly for $PM_{2.5}$ emissions, our results indicated that the $PM_{2.5}$ concentration decreased by 28.2% from 2010 to 2015. The decrease in air pollution accelerated after 2014, when straw burning was forbidden in certain areas in Henan Province. For example, the number of straw-burning events calculated by the Office of the Ministry of Environmental Protection was 37.18% lower in 2015 than in 2014 (Office of the Ministry of Environmental Protection, 2015).

In this study, we further processed the Multi-resolution Emission Inventory for China (MEIC, http://meicmodel.org) data with a spatial resolution of 0.25° × 0.25° to estimate anthropogenic emissions in the CPER. Fig. 8 shows the spatial distribution of the MEIC anthropogenic NO_x and $PM_{2.5}$ inventory in 2012. Figs. 8(a) and 8(b) show that the areas with high emissions are mainly concentrated in megacities, such as Zhengzhou, Jiaozuo, and Xinxiang, as well as in areas with high densities of industry and power plants. The $PM_{2.5}$ from residential sources, as depicted in Fig. 8(c) (2), had a very similar distribution as the transportation NO_x sources (Fig. 8(d), 1), and both were mostly concentrated in urban areas with dense populations. As shown in Table 3, we calculated the total anthropogenic emissions of NO_x and $PM_{2.5}$ in Henan in three years (2008, 2010, and 2012). For NO_x, industry, power plants, and transportation were the major sources of NO_x emissions, with each accounting for approximately one-third of the total NO_x emissions. Both industrial and power plant emissions increased from 2008 to 2010 and decreased from 2010 to 2012, suggesting a close connection to the NO_x emission-reduction measures established in the 12th Five-Year Plan (Foy *et al.*, 2016; Liu *et al.*, 2016). In contrast, the NO_x emissions from transportation increased by 4 × 10^4 t along with the increase in the number of vehicles during the four years. Unlike NO_x, anthropogenic $PM_{2.5}$ emissions are mainly contributed by industrial and residential sources, which together accounted for more than 85% of the emissions in 2012. Except for the increase in residential emissions from 2010 to 2012, the industrial, power and transportation emissions all showed significant declines from 2008 to 2012.

The monthly average concentrations of NO_2 and $PM_{2.5}$ over the CPER are shown in Fig. 9. The monthly average concentrations of NO_2 and $PM_{2.5}$ showed cyclical variation throughout the year. Low concentrations of NO_2 and $PM_{2.5}$ generally occurred during the summer, i.e., July and August. The predicted monthly average NO_2 concentration reached a minimum value of 4.39 × 10^{15} molecules cm^{-2} in July 2006, and the predicted monthly average $PM_{2.5}$ concentration reached a minimum level of 40.2 μg m^{-3} in August 2005. The peak predicted concentrations generally appeared during winter, i.e., December and January. In January 2013, both NO_2 and $PM_{2.5}$ concentrations reached their highest values of 31.68 × 10^{15} molecules cm^{-2} and 181.6 μg m^{-3}, respectively. The air quality in the CPER was also affected by the short-term emission reduction program implemented by the Chinese government during international events. For example, in Henan Province, the

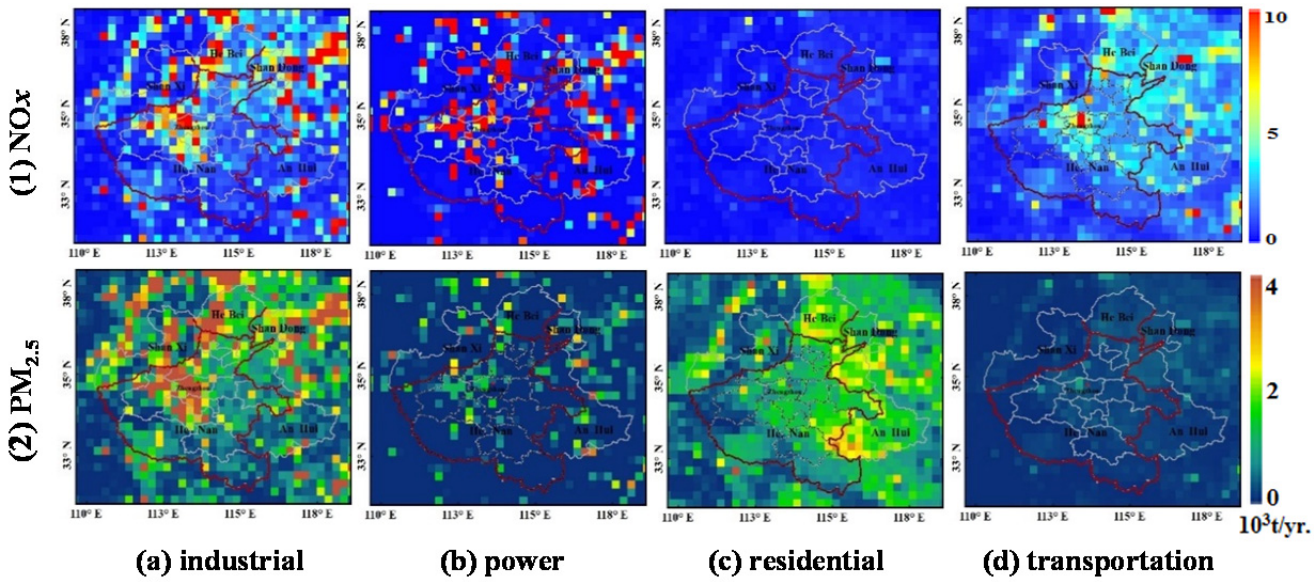

Fig. 8. Spatial distribution of the MEIC NO_x (1) and $PM_{2.5}$ (2) emissions in 2012 at 0.25° × 0.25° resolution by source: (a) industrial, (b) power, (c) residential, and (d) transportation.

Table 3. Four sources of anthropogenic NO_x and $PM_{2.5}$ emissions (i.e., industrial, power, residential and transportation) in Henan in 2008, 2010 and 2012. (Unit: 10^4 t yr^{-1}.)

Year	NO_x		$PM_{2.5}$		Type
2008	45.87	(29.34%)	51.99	(57.84%)	Industrial
2010	59.57	(34.41%)	45.09	(56.53%)	
2012	58.20	(33.68%)	40.50	(53.24%)	
2008	55.62	(35.58%)	6.14	(6.83%)	Power
2010	56.39	(32.57%)	5.22	(6.55%)	
2012	55.28	(31.99%)	4.25	(5.59%)	
2008	5.40	(3.46%)	27.11	(30.16%)	Residential
2010	5.15	(2.98%)	25.23	(31.64%)	
2012	5.64	(3.26%)	27.22	(35.79%)	
2008	49.42	(31.62%)	4.65	(5.17%)	Transportation
2010	52.00	(30.04%)	4.21	(5.28%)	
2012	53.70	(31.07%)	4.10	(5.38%)	

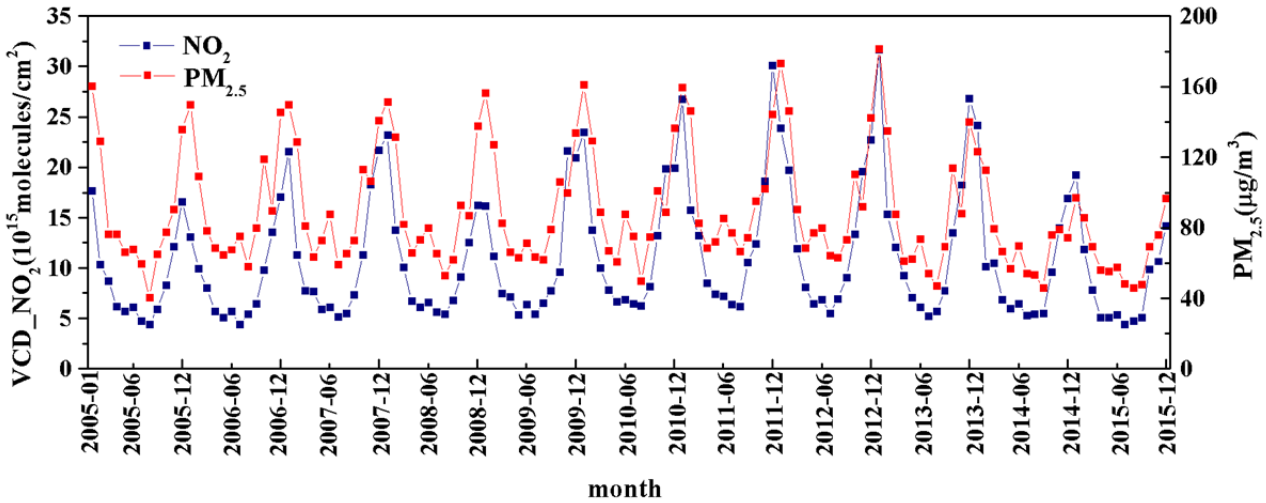

Fig. 9. The monthly variations in NO_2 columnar concentration and $PM_{2.5}$ mass concentration in the CPER during 2005–2015.

concentrations of NO_2 and $PM_{2.5}$ reached their lowest levels for the December period during the 11-year study period in December 2015 following the implementation of a short-term emission reduction program related to the Shanghai Cooperation Organization Summit, which occurred from December 14 to 16, 2015. Another example was the 2008 Beijing Summer Olympic Games. The monthly average concentrations of NO_2 in 2008 were significantly lower than those in the same period in preceding years.

The correlation analysis of NO_2 and $PM_{2.5}$ indicated that the concentrations of the two air pollutants were highly correlated (0.84) (Fig. 10). This significantly positive relationship might provide a reference for future emission control plans. Based on the current results, the control of NO_2 emissions could lead to a reduction in ambient $PM_{2.5}$ concentrations as well.

CONCLUSION

This study estimated the concentrations of NO_2 and ground-level $PM_{2.5}$ in the CPER using satellite remote sensing over 11 study years. The spatial distributions of NO_2 and $PM_{2.5}$ concentrations were examined, including the monthly and seasonal concentration variations in the CPER and in 12 core cities. The areas with high NO_2 concentrations were mainly located in eastern Hebei Province and northern Henan Province. Among the investigated cities, Jiaozuo had the highest 11-year average concentration of NO_2 (19.54×10^{15} molecules cm^{-2}). The spatial distribution of $PM_{2.5}$ is similar to that of NO_2. The city of Hebi and the surrounding area had the highest concentrations of $PM_{2.5}$ (107.8 $\mu g\ m^{-3}$). In the CPER, Sanmenxia, southwestern Luoyang, and Xinyang had lower levels of air pollution. These cities are all located in the mountainous region of Henan Province.

The predicted concentrations of NO_2 and $PM_{2.5}$ showed cyclical variations by month and season. Within a calendar year, the winter was usually associated with higher concentrations of NO_2 and $PM_{2.5}$, while summer was usually associated with lower concentrations of NO_2 and $PM_{2.5}$. Overall, the pollution levels of the four seasons were ranked as follows (in descending order): winter, autumn, spring, and summer. Fossil fuel consumption and weather were the two most important factors in the seasonal variations in air pollution in the CPER. The high demand for heating in winter increased the consumption of coal, and the static atmospheric conditions in winter prevented pollutants from dispersing. Therefore, winter had the highest air pollution levels among the four seasons.

Both the NO_2 and $PM_{2.5}$ concentrations fluctuated during the 11 years we studied, but the variation in NO_2 was greater than in $PM_{2.5}$ in the CPER. The average annual concentration of NO_2 was lowest in 2006 and then increased greatly in 2007. The average annual concentrations of NO_2 increased gradually from 2007 till 2010 and peaked in 2011. However, due to emission control efforts in recent years, the average annual concentration of NO_2 decreased in 2014 and 2015, approaching the low concentration observed in 2006. The variation in the $PM_{2.5}$ concentrations was consistent with that in the NO_2 concentrations. The average annual concentration of $PM_{2.5}$ peaked in 2012 and continued to decline over subsequent years, reaching its lowest level in 2015.

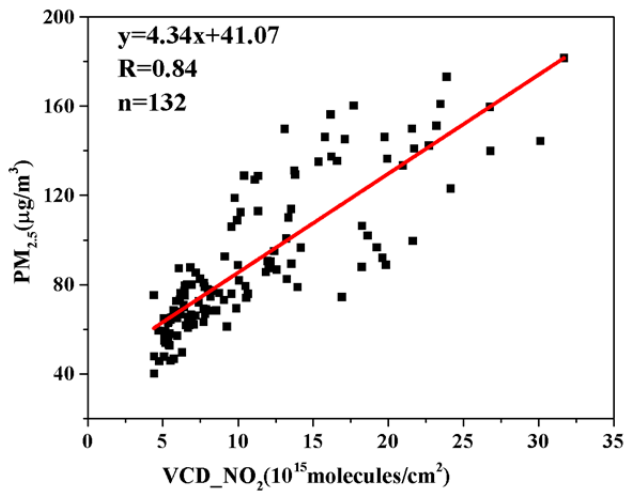

Fig. 10. Scatterplot of the monthly NO_2 columnar concentration and $PM_{2.5}$ mass concentration in the CPER during 2005–2015.

ACKNOWLEDGMENTS

This research was financially supported by the National Key R&D Program of China (2016YFC0201507) and the National Natural Science Foundation of China (grant Nos. 91543128 and 41571417). We thank NASA's Atmospheric Sciences Data Center for producing the MODIS and OMI datasets.

REFERENCES

Apte, J.S., Marshall, J.D., Cohen, A.J. and Brauer, M. (2015). Addressing global mortality from ambient $PM_{2.5}$. *Environ. Sci. Technol.* 49: 8057–8066.

Boersma, K., Eskes, H., Veefkind, J., Brinksma, E., van der, A., R., Sneep, M., van den Oord, G., Levelt, P., Stammes, P. and Gleason, J. (2007). Near-real time retrieval of tropospheric NO_2 from OMI. *Atmos. Chem. Phys.* 7: 2103–2118.

Bucsela, E.J., Krotkov, N.A., Celarier, E.A. and Lamsal, L.N. (2013). A new stratospheric and tropospheric NO_2 retrieval algorithm for nadir-viewing satellite instruments: Applications to OMI. *Atmos. Meas. Tech.* 6: 2607-2626.

CAAC (2015). *China air quality management assessment report (2015)*, Clean Air Alliance of China, Beijing.

Celarier, E.A., Brinksma, E.J., Gleason, J.F., Veefkind, J.P., Cede, A., Herman, J.R., Ionov, D., Goutail, F., Pommereau, J.P., Lambert, J.C., van Roozendael, M., Pinardi, G., Wittrock, F., Schönhardt, A., Richter, A., Ibrahim, O.W., Wagner, T., Bojkov, B., Mount, G., Spinei, E., Chen, C.M., Pongetti, T.J., Sander, S.P., Bucsela, E.J., Wenig, M.O., Swart, D.P.J., Volten, H., Kroon, M. and Levelt, P.F. (2008). Validation of ozone

monitoring instrument nitrogen dioxide columns. *J. Geophys. Res.* 113: D15S15.

Cheng, Y., Engling, G., He, K.B., Duan, F.K., Ma, Y.L., Du, Z.Y., Liu, J.M., Zheng, M. and Weber, R.J. (2013). Biomass burning contribution to Beijing aerosol. *Atmos. Chem. Phys.* 13: 7765–7781.

de Foy, B.D., Lu, Z. and Streets, D.G. (2016). Satellite NO_2 retrievals suggest china has exceeded its NO_x reduction goals from the twelfth five-year plan. *Sci. Rep.* 6: 35912.

Duki, M.I., Sudarmadi, S., Suzuki, S., Kawada, T. and Tri-Tugaswati, A. (2003). Effect of air pollution on respiratory health in Indonesia and its economic cost. *Arch. Environ. Health* 58: 135–143.

Fengxia, G., Min, B., Yijun, M., Zupei, L., Yawen, L. and Haifeng, S. (2016). Temporal and spatial characteristics of lightning-produced nitrogen oxides in China. *J. Atmos. Sol. Terr. Phys.* 149: 100–107.

Gu, D., Wang, Y., Smeltzer, C. and Liu, Z. (2013). Reduction in NO_x Emission trends over China: Regional and seasonal variations. *Environ. Sci. Technol.* 47: 12912–12919.

Guo, F.X., Ju, X.Y., Bao, M., Lu, G.Y., Liu, Z.P., Li, Y.W. and Mu, Y.J. (2017). Relationship between lightning activity and tropospheric nitrogen dioxide and the estimation of lightning-produced nitrogen oxides over China. *Adv. Atmos. Sci.* 34: 235–245.

Ialongo, I., Herman, J., Krotkov, N., Lamsal, L., Folkert Boersma, K., Hovila, J. and Tamminen, J. (2016). Comparison of OMI NO_2 observations and their seasonal and weekly cycles with ground-based measurements in Helsinki. *Atmos. Meas. Tech.* 9: 1–13.

Irie, H., Muto, T., Itahashi, S., Kurokawa, J. and Uno, I. (2016). Turnaround of tropospheric nitrogen dioxide pollution trends in China, Japan, and South Korea. *SOLA* 12: 170–174.

Itahashi, S., Uno, I., Irie, H., Kurokawa, J.I. and Ohara, T. (2014). Regional modeling of tropospheric NO_2 vertical column density over East Asia during the period 2000-2010: Comparison with multisatellite observations. *Atmos. Chem. Phys.* 14: 3623–3635.

Jin, J., Ma, J., Lin, W., Zhao, H., Shaiganfar, R., Beirle, S. and Wagner, T. (2016). MAX-DOAS measurements and satellite validation of tropospheric NO_2 and SO_2 vertical column densities at a rural site of north China. *Atmos. Environ.* 133: 12–25.

Khoder, M.I. (2002). Atmospheric conversion of sulfur dioxide to particulate sulfate and nitrogen dioxide to particulate nitrate and gaseous nitric acid in an urban area. *Chemosphere* 49: 675–684.

Krotkov, N.A., Mclinden, C.A., Li, C., Lamsal, L.N., Celarier, E.A., Marchenko, S.V., Swartz, W.H., Bucsela, E.J., Joiner, J., Duncan, B.N., Boersma, K.F., Veefkind, J.P., Levelt, P.F., Fioletov, V.E., Dickerson, R.R., He, H., Lu, Z. and Streets, D.G. (2016). Aura omi observations of regional SO_2 and NO_2 pollution changes from 2005 to 2015. *Atmos. Chem. Phys.* 16: 4605–4629.

Levy, R.C., Mattoo, S., Munchak, L.A., Remer, L.A., Sayer, A.M., Patadia, F. and Hsu, N.C. (2013). The Collection 6 MODIS aerosol products over land and ocean. *Atmos. Meas. Tech.* 6: 2989–3034.

Li, D., Guo, Y., Li, Y., Ding, P., Wang, Q. and Cao, Z. (2012). Air pollutant emissions from coal-fired power plants. *Open J. Air Pollut.* 1: 37–41.

Li, L., Wang, Y., Zhang, Q., Li, J., Yang, X. and Jin, J. (2008). Wheat straw burning and its associated impacts on Beijing air quality. *Sci. China Ser. D* 51: 403–414.

Li, S., Yu, C., Chen, L., Tao, J., Letu, H., Ge, W., Si, Y. and Liu, Y. (2016). Inter-comparison of model-simulated and satellite-retrieved componential aerosol optical depths in china. *Atmos. Environ.* 141: 320–332.

Lin, J.T., Martin, R.V., Boersma, K.F., Sneep, M., Stammes, P., Spurr, R., Wang, P., Van Roozendael, M., Clémer, K. and Irie, H. (2014). Retrieving tropospheric nitrogen dioxide over china from the ozone monitoring instrument: Effects of aerosols, surface reflectance anisotropy and vertical profile of nitrogen dioxide. *Atmos. Chem. Phys.* 14: 1441–1461.

Liu, F., Zhang, Q., van der A, R.J., Zheng, B., Tong, D., Yan, L., Zheng, Y. and He, K. (2016). Recent reduction in NO_x emissions over China: Synthesis of satellite observations and emission inventories. *Environ. Res. Lett.* 11: 114002.

Ma, Z., Hu, X., Sayer, A.M., Levy, R., Zhang, Q., Xue, Y., Tong, S., Bi, J., Huang, L. and Liu, Y. (2016). Satellite-based spatiotemporal trends in $PM_{2.5}$ concentrations: China, 2004-2013. *Environ. Health Perspect.* 124: 184–192.

Ministry of Environmental Protection (2017). http://www.zhb.gov.cn/gkml/hbb/qt/201704/t20170405_409362.htm.

Miyazaki, K., Eskes, H.J., Sudo, K. and Zhang, P.M.C. (2014). Global lightning NO_x production estimated by an assimilation of multiple satellite data sets. *Atmos. Chem. Phys.* 13: 29203–29261.

Natural Resources Defense Council (NRDC) (2015). *China coal consumption cap plan and research report: Recommendations for the 13th five-year plan.* Natural Resources Defense Council, Beijing, China.

Office of the Ministry of Environmental Protection (2014). http://www.zhb.gov.cn/gkml/hbb/bgth/201409/t20140918_289253.htm, Last Access: 15 September 2014.

Office of the Ministry of Environmental Protection (2015). http://www.pkulaw.cn/fulltext_form.aspx?gid=258287, Last Access: 10 August 2015.

Pope, C.A. and Dockery, D.W. (2006). Health effects of fine particulate air pollution: Lines that connect. *J. Air Waste Manage. Assoc.* 56: 709–742.

Russell, A.R., Valin, L.C. and Cohen, R.C. (2012). Trends in OMI NO_2 observations over the United States: Effects of emission control technology and the economic recession. *Atmos. Chem. Phys.* 12: 12197–12209.

Streets, D.G., Canty, T., Carmichael, G.R., de Foy, B., Dickerson, R.R., Duncan, B.N., Edwards, D.P., Haynes, J.A., Henze, D.K., Houyoux, M.R., Jacob, D.J., Krotkov, N.A., Lamsal, L.N., Liu, Y., Lu, Z., Martin, R.V., Pfister, G.G., Pinder, R.W., Salawitch, R.J. and Wecht, K.J. (2013). Emissions estimation from satellite retrievals: A review of current capability. *Atmos. Environ.* 77:

1011–1042.

Sun, L., Li, R., Tian, X. and Wei, J. (2017). Analysis of the temporal and spatial variation of aerosols in the Beijing-Tianjin-Hebei region with a 1 km AOD product. *Aerosol Air Qual. Res.* 17: 923–935.

Tian, H., Wang, Y., Zhao, D., Chai, F., Xing, Z. and Cheng, K. (2011). Formation and causes of NO_x pollution on the east side of the Taihang Mountains in China. *Chin. Sci. Bull.* 56: 2044–2049.

United States Environmental Protection Agency (USEPA) (2010). *Our nation's air status and trends through 2008*, EPA-454/R-09e002, Research Triangle Park, North Carolina, USA.

van der A, R.J., Peters, D.H.M.U., Eskes, H., Boersma, K.F., Van Roozendael, M., De Smedt, I. and Kelder, H.M. (2006). Detection of the trend and seasonal variation in tropospheric NO_2 over China. *J. Geophys. Res.* 111: D12317.

Van Donkelaar, A., Martin, R.V. and Park, R.J. (2006). Estimating ground-level $PM_{2.5}$ using aerosol optical depth determined from satellite remote sensing. *J. Geophys. Res.* 111: D21201.

Van Donkelaar, A., Martin, R.V., Brauer, M., Kahn, R., Levy, R., Verduzco, C. and Villeneuve, P.J. (2015). *Global estimates of ambient fine particulate matter concentrations from satellite-based aerosol optical depth: Development and application*, University of British Columbia, Canada.

Wang, S., Xing, J., Chatani, S., Hao, J., Klimont, Z., Cofala, J. and Amann, M. (2011). Verification of anthropogenic emissions of china by satellite and ground observations. *Atmos. Environ.* 45: 6347–6358.

Wang, S.W., Zhang, Q., Streets, D.G. and He, K.B. (2012). Growth in NO_x emissions from power plants in China: Bottom-up estimates and satellite observations. *Atmos. Chem. Phys.* 12: 45–91.

Wang, S.X. and Hao, J.M. (2012). *Emissions of air pollutants from power plants in China*, Tsinghua University, Beijing, China.

Wang, Y., McElroy, M.B., Boersma, K.F., Eskes, H.J. and Veefkind, J.P. (2007). Traffic restrictions associated with the Sino-African summit: Reductions of NO_x detected from space. *Geophys. Res. Lett.* 34: 402–420.

Wang, Y., Ying, Q., Hu, J. and Zhang, H. (2014a). Spatial and temporal variations of six criteria air pollutants in 31 provincial capital cities in China during 2013-2014. *Environ. Int.* 73: 413–422.

Wang, Y., Zhang, R.Y. and Saravanan, R. (2014b). Asian pollution climatically modulates midlatitude cyclones following hierarchical modeling and observational analysis. *Nat. Commun.* 5: 3098.

Wenig, M.O., Cede, A.M., Bucsela, E.J., Celarier, E.A., Boersma, K.F., Veefkind, J.P., Brinksma, E.J., Gleason, J.F. and Herman, J.R. (2008). Validation of OMI tropospheric NO_2 column densities using direct-sun mode brewer measurements at NASA Goddard Space Flight Center. *J. Geophys. Res.* 113: D16S45.

West, J.J., Cohen, A., Dentener, F., Brunekreef, B., Zhu, T., Armstrong, B., Bell, M.L., Brauer, M., Carmichael, G., Costa, D.L., Dockery, D.W., Kleeman, M., Krzyzanowski, M., Künzli, N., Liousse, C., Lung, S.C., Martin, R.V., Pöschl, U., Pope, Pope, C.A., Roberts, J.M., Russell, A.G. and Wiedinmyer, C. (2016). What we breathe impacts our health: Improving understanding of the link between air pollution and health. *Environ. Sci. Technol.* 50: 4895–4904.

Yan, H.H., Zhang, X.Y. and Wang, W.H. (2015). Spatiotemporal variations of NO_2 and SO_2 over global region and China by OMI observations during 2004-2014. *Sci. Technol. Rev.* 33: 41–51.

Yao, L. and Lu, N. (2014). Spatiotemporal distribution and short-term trends of particulate matter concentration over China, 2006-2010. *Environ. Sci. Pollut. Res. Int.* 21: 9665–9675.

Zhang, H., Yu, C., Su, L., Li, L., Fan, M., Wang, Y. and Chen, L. (2017a). MODIS and OMI data to assess the effectiveness of atmospheric emissions reduction during the parade 2015 in Beijing. *J. Remote Sens.* 21: 622–632.

Zhang, L., Lee, C.S., Zhang, R. and Chen, L. (2017b). Spatial and temporal evaluation of long term trend (2005–2014) of OMI retrieved NO_2 and SO_2 concentrations in Henan Province, China. *Atmos. Environ.* 154: 151–166.

Zhang, R.J., Tao, J., Ho, K.F., Shen, Z.X., Wang, G.H., Cao, J.J. (2012). Characterization of atmospheric organic and elemental carbon of $PM_{2.5}$ in a typical semi-arid area of northeastern China. *Aerosol Air Qual. Res.* 12: 792–802.

Zhang, X.Y., Zhang, P., Zhang, Y., Li, X.J. and Qiu, H. (2007). Variation trend, temporal and spatial distribution characteristics and source apportionment of tropospheric NO_2 over 10A in China. *Chin. Sci. D* 37: 1409–1416.

Zhang, Y., Pun, B., Wu, S.Y., Vijayaraghavan, K. and Seigneur, C. (2004). Application and evaluation of two air quality models for particulate matter for a Southeastern U.S. episode. *J. Air Waste Manage. Assoc.* 54: 1478–1493.

Zhang, Y.L. and Cao, F. (2015). Fine particulate matter ($PM_{2.5}$) in China at a city level. *Sci. Rep.* 5: 14884.

Zhao, B., Wang, S.X., Liu, H., Xu, J.Y., Fu, K., Klimont, Z., Hao, J.M., He, K.B., Cofala, J. and Amann, M. (2013). NO_x emissions in China: Historical trends and future perspectives. *Atmos. Chem. Phys.* 13: 9869–9897.

Zhao, S., Yu, Y., Yin, D., He, J., Liu, N., Qu, J. and Xiao, J. (2016). Annual and diurnal variations of gaseous and particulate pollutants in 31 provincial capital cities based on in situ air quality monitoring data from China national environmental monitoring center. *Environ. Int.* 86: 92–106.

Zhou, C.Y., Li, Q., He, Y.X., Wang, Z.T., Chen, H., Zhang, L.J., Mao, H.Q. and Yu, C. (2015). Spatial-temporal change of troposphere NO_2 column density and its impact factors over Shandong Province. *China Environ. Sci.* 35: 2281–2290.

Zhou, C.Y., Li, Q., Wang, Z.T., Gao, Y.H., Zhang, L.J., Chen, H., Ma, P.F. and Tan, C. (2016a). Spatial-temporal trend and changing factors of troposphere NO_2 column density in Beijing-Tianjin-Hebei region from 2005 to 2014. *J. Remote Sens.* 20: 468–480.

Zhou, C.Y., Wang, Q., Li, Q., Liu, S.H., Chen, H., Ma, P.F., Wang, Z.T. and Tan, C. (2016b). Spatio-temporal change and influencing factors of tropospheric NO_2 column density of Yangtze River delta in the decade. *China Environ. Sci.* 36: 1921–1930.

Received for review, October 17, 2017
Revised, March 29, 2018
Accepted, March 30, 2018